

# Synthesis and Characterization of Silver Nanoparticle Rings Embedded in Glass

Y. Chen\*, J. Jaakola\*, Y.L. Ge\*\*, A. Säynätjoki\*, A. Tervonen\*, S. Hannula\*\*, and S. Honkanen\*

\* Helsinki University of Technology, Department of Micro and Nanosciences  
Micronova, Tietotie 3, FIN-02015 Espoo, Finland, ya.chen@tkk.fi

\*\* Helsinki University of Technology, Department of Materials Science and Engineering  
P.O. Box 6200, FI-02015 Espoo, Finland

## ABSTRACT

Silver nanoparticle rings embedded in glass are fabricated by ion exchange technique with photolithographically patterned metal mask. Optical transmission measurement is performed to characterize the optical properties of silver nanoparticles. Atomic force microscopy (AFM) of an etched sample further shows the pattern of the nanoparticles. Transmission electron microscope (TEM) with X-ray energy dispersive spectroscopy (EDS) and electron diffraction pattern are utilized to observe cross-sectional distribution and to confirm the existence of silver. The results indicate that the masked ion exchange process can provide the possibility of making patterned nanoparticle formations to be used in e. g. surface enhanced spectroscopy.

**Keywords:** silver nanoparticles, ion exchange, glass waveguides

## 1 INTRODUCTION

Metallic nanoclusters with their unique optical properties have generated great interests in many fields such as biological sensing, nanophotonic devices [1], [2]. Previously, the glass materials containing silver nanoclusters have been prepared by light-ion irradiation and annealing of ion exchanged glasses [3]. However, because of processing limitations such as the lack of a patterning method of nanoparticles, and post processing induced defects, these methods have not been developed to their full potential yet. Low energy diffusive ion exchange technique with standard photolithography procedure is well-known for making optical waveguides [4]–[6]. It has been found that some silver nanoparticles are introduced in this process; however, they are removed for reducing absorption and scattering losses when making high quality waveguides [7]. Here we report on utilizing the low energy diffusive ion exchange technique and intentionally enhancing the nanoparticle generation to fabricate patterned silver nanoparticle formations embedded in glass without any post processing. These localized patterns of nanoparticles can be compatible with potassium-exchanged waveguides [8] and microfluidic channels [9] into an integrated chip for high-sensitivity surface enhanced spectroscopy.

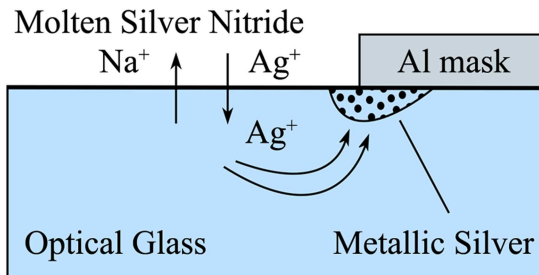


Figure 1: Electrolytic deposition of silver beneath the edge of the aluminum mask during ion exchange.

In silver-sodium ion exchange utilizing lithographically patterned metal mask films, metallic silver is found to be buried inside the glass after silver ion exchange and the affected area is limited to the direct vicinity of the mask edge. The electrolytic deposition principle, as described earlier [10], is illustrated in Fig. 1. In ion exchange system an electric potential arises because more sodium diffuses out of the glass than silver diffuses in, since sodium ions are more active and mobile than silver ions. This results in an electrical potential different from the electrochemical potential between the aluminum mask and the melt which in turn leads to an ionic current that will flow as illustrated in Fig. 1. In the regions close to the mask edge, unbalanced excess silver is reduced as metallic material. Therefore, the deposition of clusters of metallic silver is a direct consequence of the ionic current flow. The previous research indicates the distance between the patterns changes the resistance of the aluminum mask and eventually influences the amount of metallic silver deposition.

## 2 EXPERIMENTAL

The silver nanoparticle rings were fabricated by silver ion exchange procedure with a photolithographic mask. First, an aluminum film was evaporated on the glass substrate (Corning 0211) and the pattern of the mask was obtained by standard photolithography procedure. The masked glass wafers were dipped into a molten mixture of 5%  $AgNO_3$  in a 50/50 mixture of  $KNO_3$  and  $NaNO_3$  in a crucible furnace heated at 300 °C for 6 h. For forming silver nanoparticle rings, the features on

the mask were circular holes with diameters as 4 and 10  $\mu\text{m}$ , spacing widths changing from 15 to 250  $\mu\text{m}$ .

For optical transmission measurements, the aluminum films were removed by etching. The light source covering the ultraviolet and visible range of the spectrum was used to illuminate the sample. The studied features were the circular holes with 10  $\mu\text{m}$  in diameter and different spacing widths. They were magnified by a microscope objective (60X, NA = 0.55) and the measured area was limited by an aperture. The transmitted light was split into two branches by a flipping mirror: one was connected to a CCD camera for imaging the pattern and checking the feature position, and the other one was connected to a spectrometer for obtaining the spectrum.

To observe the silver nanoparticle rings embedded in glass, the sample was dipped into the  $\text{SiO}_2$  etchant for 1 minute to remove a 55 nm thick glass layer from the surface. Then, atomic force microscopy (AFM) analysis of the exposed nanoparticle rings was performed to obtain the lateral distribution.

In order to observe the cross-sectional distribution of silver nanoparticles along the pattern edge, focused ion beam (FIB) technique was employed for preparing a transmission electron microscopy (TEM) specimen [11]. A 100 nm copper (Cu) layer was deposited on the top of the substrate to avoid electron-beam induced charging problem, and a 1.5  $\mu\text{m}$  platinum (Pt) layer was deposited to protect sample surface and to avoid curtain effects during the procedure. Then, we fabricated the electron-transparent lamella via FIB milling and lifted the lamella using an Omniprobe nanomanipulator. The specimen was glued on a lift-off grid by Pt deposition, and finally thinned down to a desired thickness. Transmission electron microscopy (TEM) with X-ray energy dispersive spectroscopy (EDS) and electron diffraction pattern are utilized to observe cross-sectional distribution and to confirm the existence of silver.

### 3 RESULTS AND DISCUSSION

The optical transmission spectra of the ion-exchanged 10- $\mu\text{m}$  circular patterns with different spacings are shown in Fig. 2. The reference spectrum is from a fully masked area of the sample. The peak position of the optical response of the matrix-embedded silver nanoparticles is observed to be around 400 nm, which is identified as surface plasmon resonance (SPR) of silver. In Fig. 2, with increasing pattern spacing, therefore reducing the resistance of the aluminum film and increasing the ion current and the deposited silver, the transmission increases as the same trend. For 10  $\mu\text{m}$ -circle, the increasing trend is not obvious when the spacing width is above 100  $\mu\text{m}$ .

Fig. 3 shows AFM images of regions ion-exchanged through a 4  $\mu\text{m}$  circular opening, with two different

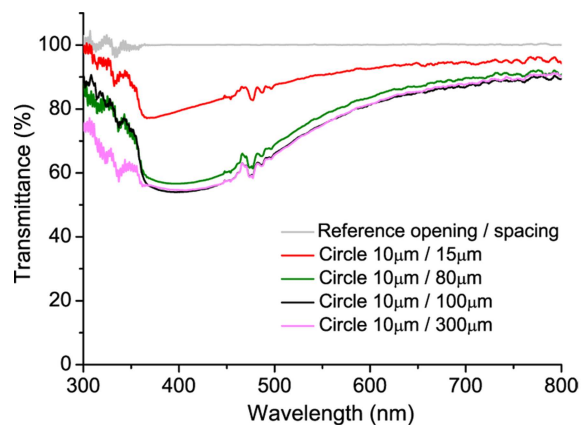


Figure 2: Transmission spectra of silver nanoparticles for 10- $\mu\text{m}$  circular patterns with different spacings.

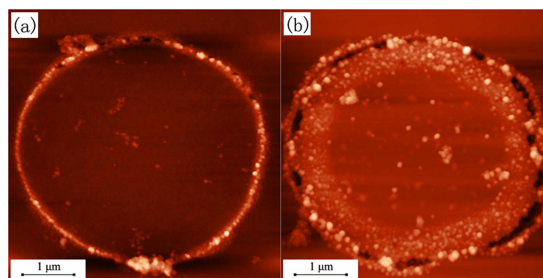


Figure 3: The pattern observed by AFM. (a) The ring with 4  $\mu\text{m}$  opening and 15  $\mu\text{m}$  spacing. (b) The ring with 4  $\mu\text{m}$  opening and 100  $\mu\text{m}$  spacing.

spacings between openings. These images show that more nanoparticles are formed for the same mask opening size having larger spacing, which is in a good match with the transmission spectra in Fig. 1. And AFM images of etched sample give a clear way to demonstrate the silver nanoparticle rings embedded in glass.

Fig. 4(a) shows the TEM image of the cross-sectional underneath the mask edge of a 10- $\mu\text{m}$  circle pattern. A bright field TEM image of these silver nanoparticles with higher magnification and their electron diffraction pattern are given in Fig. 4(b) and Fig. 4(c). The average size of the particles is estimated to be 5 to 10 nm, and some of them aggregate together to form larger clusters. The electron diffraction pattern from this area is indexed as cubic silver to prove the crystalline metallic structure of the nanoparticles. In addition, as shown in Fig. 4(d), X-ray energy dispersive spectroscopy (EDS) gives the element analysis from the sample. The measurements from TEM give the cross-section distribution of silver nanoparticles. In particular, the TEM image shows that the most dense nanoparticle formations are not at the interface of Al mask and glass surface, but at a distance of some 50-100 nm below it. This is different from the

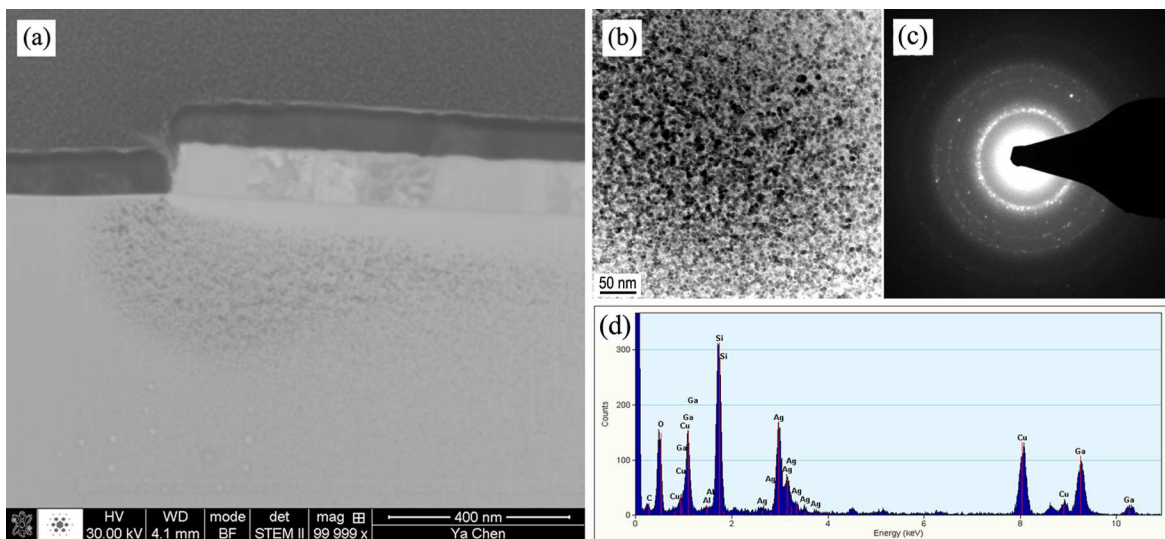


Figure 4: (a) The overview image of silver nanoparticles underneath mask edge for 10- $\mu$ m circular pattern. (b) Bright field image of silver nanoparticles. (c) The electron diffraction pattern from area in (b). (d) EDS spectrum of element analysis of the nanoparticles. (The elements other than Ag in the spectrum are from: Pt-deposit layer, Cu-deposit layer and TEM grid, Al-mask, Ga-focused ion beam, Si/O-glass.)

expectations from the qualitative model described above for forming of nanoparticles [10]. Explanation for this feature may still require further study, before a more complete model can be established. It is noted, that this distribution of silver nanoparticles found in TEM images, resembles the modeled silver concentration distributions under the metal mask edges in ion-exchanged waveguides in an earlier work [12]. This model used special boundary conditions under the mask, based on the disturbing effect of the conducting mask layer on the electric field normally arising in glass with gradient of silver/sodium ions, which have different mobilities. As a result, silver ions were prevented from diffusing to the glass surface below the mask and silver-exchanged region was kept at some depth below the mask, similar to the location of nanoparticles in Fig. 4(a). It is a possibility that exchanged ion distribution under the mask can thus induce an electric field in glass due to charge redistribution in the metal mask, that will have an effect on ion transport and also on reduction of silver ions into metal nanoparticles.

#### 4 CONCLUSION

In conclusion, silver nanoparticle rings embedded in glass have been fabricated by ion exchange technique and standard photolithography procedure without any annealing or irradiation processing. Optical transmission measurement, TEM analysis, and AFM scans have been utilized to characterize the optical properties of silver nanoparticles, and to observe their spatial distribution. The experimental results demonstrate that pho-

tolithography masking prior to the ion exchange process can provide, not only the possibility of making patterned nanoparticles, but also a way to control nanoparticle growth and distribution.

This research is supported by the Academy of Finland under the grant 216583.

#### REFERENCES

- [1] S. M. Nie and S. R. Emory, "Probing single molecules and single nanoparticles by surface-enhanced Raman scattering," *Science* 275, 1102, 1997.
- [2] Maier, S. A. and H. A. Atwater, "Plasmonics: Localization and guiding of electromagnetic energy in metal/dielectric structures," *J. Appl. Phys.* 98(1), 011101, 2005.
- [3] J. Zhang, W. Dong, J. W. Sheng, J. W. Zheng, J. Li, L. Qiao, and L. Q. Jiang, "Silver nanoclusters formation in ion-exchanged glasses by thermal annealing, UV-laser and X-ray irradiation," *J. Cryst. Growth* 310(1), 234, 2008.
- [4] S. Yliniemi, Q. Wang, J. Albert, and S. Honkanen, "Studies on passive and active silver-sodium ion-exchanged glass waveguides and devices," *Mat. Sci. Eng. B-Solid* 149, 152, 2008.
- [5] Xesús Prieto-Blanco, "Electro-diffusion equations of monovalent cations in glass under charge neutrality approximation for optical waveguide fabrication," *Opt. Mater.* 31, 418, 2008.
- [6] A. Quaranta, E. Cattaruzza, and F. Gonella,

"Modelling the ion exchange process in glass: Phenomenological approaches and perspectives," *Mat. Sci. Eng. B-Solid* 149, 133, 2008.

- [7] J. Z. Zou and R. T. Chen, "Improvement of two-step  $K^+$ - $Na^+$  and  $Ag^+$ - $Na^+$  ion-exchanged glass waveguides by surface removal," *Appl. Phys. Lett.* 88(8), 081102, 2006.
- [8] S. Honkanen, P. Poyhonen, A. Tervonen, S. I. Najafi, "Waveguide coupler for potassium-ion-exchanged and silver-ion-exchanged wave-guides in glass," *Appl. Opt.* 32, 2109, 1993.
- [9] L. N. Jiang and S. Pau, "Integrated waveguide with a microfluidic channel in spiral geometry for spectroscopic applications," *Appl. Phys. Lett.* 90(11), 111108, 2007.
- [10] R. G. Walker, C. D. W. Wilkinson, and J. A. H. Wilkinson, "Integrated optical waveguiding structures made by silver ion-exchange in glass," *Appl. Opt.* 22(12), 1923, 1983.
- [11] Z. Rahman, S. Shukla, H. Cho and S. Seal, "In-situ site-selective FIB for high resolution TEM sample preparation," *Microscopy and Analysis* 20(3), 9, 2006.
- [12] C. D. W. Wilkinson, R. G. Walker, "The diffusion profile of stripe optical waveguides formed by ion exchange," *Electron. Lett.* 14(18), 599 (1978).